

Baeyer-Villiger oxidation of cyclopentanone over zeolite Y entrapped transition metal-Schiff base complexes

Chetan K. Modi  | Naresh Solanki | Ravi Vithalani | Dikin Patel

Applied Chemistry Department, Faculty of Technology & Engineering, The Maharaja Sayajirao University of Baroda, Vadodara 390 001 Gujarat, India

Correspondence

Chetan K. Modi, Applied Chemistry Department, Faculty of Technology & Engineering, The Maharaja Sayajirao University of Baroda, Vadodara, Gujarat, India.
Email: chetank.modi1@gmail.com

Funding information

University Grants Commission, Grant/Award Number: 42-290/2013 (SR) dated-25th March, 2013; UGC, New Delhi, Grant/Award Number: 42-290/2013

Transition metal [M = VO (IV) and/or Cu (II)] complexes with Schiff base ligand, (Z)-2-((2-hydroxybenzylideneamino)phenol) (H₂L) have been entrapped in the super cages of zeolite-Y by Flexible Ligand Method. Synthesized materials have been characterized by preferential physico-chemical techniques such as inductively coupled plasma optical emission spectroscopy (ICP-OES), elemental analyses (CHN), fourier transmission infrared spectroscopy (FTIR), electronic and UV-reflectance spectra, Brunauer–Emmett–Teller (BET) surface area measurements, scanning electron micrographs (SEMs), X-ray diffraction patterns (XRD) and thermogravimetric analysis (TGA). The catalytic competence of zeolite-Y entrapped transition metal complexes was examined in Baeyer-Villiger (BV) oxidation of cyclopentanone using 30% H₂O₂ as an oxidant beside neat complexes to check the aptitude of heterogeneous catalysis over the homogeneous system. The effect of experimental variables such as mole ratio of substrate to an oxidant, amount of catalyst, reaction time, varying oxidants and solvents on the conversion of cyclopentanone was also tested. Under the optimized reaction conditions, one of the zeolite-Y entrapped transition metal complex viz. [VO(L)H₂O]-Y [where L = (Z)-2-((2-hydroxybenzylideneamino)phenol)] was found to be a potential contender by providing 80.22% conversion of cyclopentanone (TON: 10479.42), and the selectivity towards δ -valerolactone was 83.56%.

KEYWORDS

Baeyer-Villiger oxidation of cyclopentanone, flexible ligand method, heterogeneous catalysts, zeolite-Y entrapped transition metal complexes

1 | INTRODUCTION

For chemical transformation in both academia and industry, catalyst technology is nowadays used as a powerful tool because it plays a vital role in chemical reactions, allowing faster conversion of a wide variety of starting material to high-value products at lower cost with minimum generation of by-product. In this day and age, the meadow of heterogeneous catalysts has pulled up as eco-sustainable catalytic systems transforming various organic substrates into valuable intermediates for environmentally benign industrial processes due to its high stability, activity and effortless separation

from reaction mixtures. On the other hand, homogeneous systems are often regarded as imprecise with many restrictions, including the decomposition and deactivation due to the formation of dimeric μ -oxo- and peroxy- bridged species, and separation problem as well.^[1] With added benefits of flexibility in immobilization of various chemical moieties and/or nanomaterials into the reaction channels, molecular sieves have been expanded into an imposing group of inorganic-crossbreed materials (active heterogeneous catalysts) with huge number of industrial applications, mainly in the field of catalysis. It comprises zeolites, mesoporous materials, and metal-organic frameworks. Predominantly, zeolites

are crystalline aluminosilicates formed by nanocavities and channels of strictly regular dimensions in conjunction with having assorted sizes and shapes as well. Especially, three dimensional network structure with spacious internal super cage ($\sim 13 \text{ \AA}$) and large pore diameter ($\sim 7.4 \text{ \AA}$) of zeolite-Y has been studied here as host lattices. It acquires properties like high surface area, tunable pore size and functionality, crystalline open structures, high adsorption capacity, and partitioning of reactant/products, which allows considering them as potential supports for entrapment of catalytically active complexes^[2--4] or metal complexes.^[5--8] These inorganic-crossbred porous framework compounds not only possess heterogeneous catalytic physiognomies, but also conserve high catalytic efficacy originating in homogeneous catalysis due to the site sheltered effect.^[9]

In the new born era, oxidation reactions play a vital role in many fields that benefit the chemical industries for the manufacture of high tonnage commodities, high-value fine chemicals, chemical intermediates and the pharmaceuticals.^[10--12] For instance, Baeyer-Villiger (BV) reaction is a significant oxidation process, providing a straight corridor to oxidize ketones to lactones or esters by organic peracids; and they are hefty industrial intermediates, with significance on the production of high valuable fine chemicals (e.g., steroids, antibiotics, antiviral and antiproliferative agents).^[13--20] Consequently, the development of efficient and sustainable preparative methods to access these related skeletons are of enormous importance in synthetic organic chemistry. In these days, the industrial processes engage with the use of various oxidants including perbenzoic acid,^[21] *m*-chloroperbenzoic acid (mCPBA)^[22] and trifluoroperacetic acid,^[23] which are expensive, hazardous, and possibly explosive and produces massive amount of the corresponding carboxylic acids as waste as well, which restricts their use. Furthermore, the acid by-product can diminish ester selectivity by redundant side-reactions.^[24] On the other hand, catalysts are imposed for an active transfer of oxygen to the substrate when oxidants akin to hydrogen peroxide (H_2O_2) and/or molecular O_2 are chosen. In particular, H_2O_2 is a beneficial oxidant for this reaction as it produces H_2O as the only by-product,^[25--28] which gratifies the requirements of environmentally benign approaches.

Presently, the concurrent growth in the field of heterogeneous catalysis are mainly centering on the and entrapment of metal complexes either on the inert supports or in nanovoids of zeolite Y.^[29--32] Especially, Lunsford's and Ben Taarit's groups^[33] have explored this noteworthy field of zeolite Y encapsulated transition metal complexes way back in 1970's, and is the subject that still motivating us and remained as a foremost area of catalysis.^[29--32] In connection to our earlier work,^[34--36] herein we report the liquid phase catalytic oxidation of cyclopentanone over VO(IV) and/or Cu(II) based neat and zeolite Y entrapped complexes as

catalysts using 30% H_2O_2 as an oxygen donor. The plausible mechanism of homogeneously catalyzed heterogenized Baeyer-Villiger oxidation of cyclopentanone is proposed in Scheme 1.

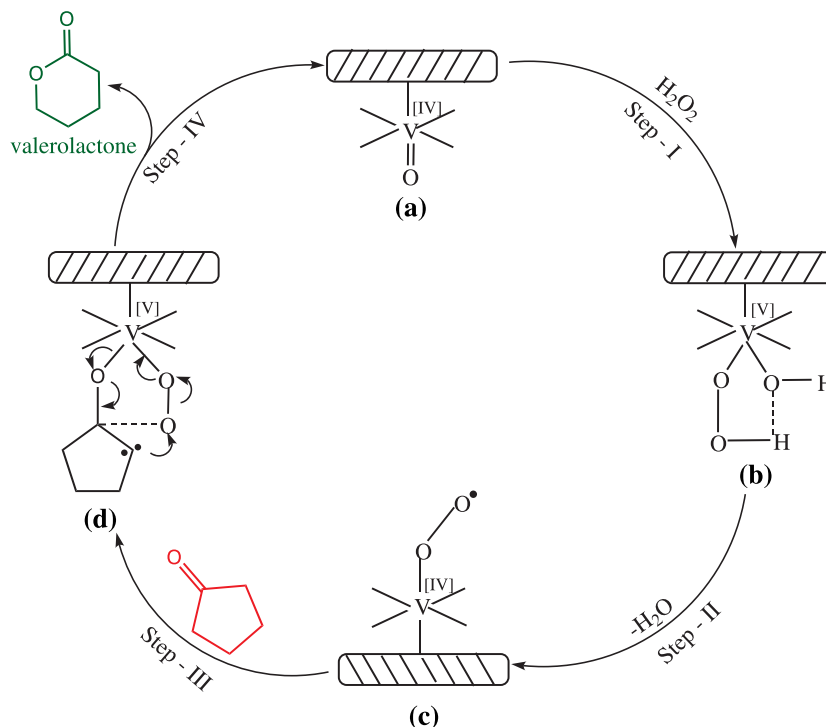
2 | EXPERIMENTAL

2.1 | Materials

All the solvents used during the synthesis of catalysts were purified by standard procedures prior to their use. Salicylaldehyde, *o*-amino phenol, 30% H_2O_2 as an oxidant, $\text{VOSO}_4 \cdot 5\text{H}_2\text{O}$ and $\text{Cu}(\text{NO}_3)_2 \cdot 3\text{H}_2\text{O}$ were purchased from Chemdyes Corporation, India. Sodium form of zeolite-Y was procured from Hi-media, India.

2.2 | Physical methods and analysis

Numerous physico-chemical methods have been employed to characterize the structure of Schiff base ligand as well as their neat and zeolite-Y entrapped VO(IV) and/or Cu(II) complexes. The quantitative analysis of Si, Al and transition metal ions of zeolite-Y entrapped complexes were carried out by ICP-OES using a model Perkin Elmer optima 2000 DV. BET surface area and pore volume of Na-Y, VO(IV)-Y, Cu(II)-Y and [VO(L)H₂O]-Y and/or [Cu(L)H₂O]-Y were measured by multipoint BET method using Micromeritics, ASAP 2010 surface area analyzer. Prior to the BET measurements, the sample was degasified at 125 °C for 2 h to remove any adsorbed gases. Scanning electron micrographs (SEMs) of zeolite-Y entrapped complexes before and after Soxhlet extraction were carried out using a SEM instrument (model: JSM-5610LV), JEOL to analyze the morphology of the samples. FTIR (4000–400 cm^{-1}) of H_2L , neat and entrapped VO(IV) and/or Cu(II) complexes were recorded with KBr pallets on the model: FTIR-8400S Shimadzu. The crystallinity of compounds was ensured by powder XRD patterns using Bruker AXS D8 Advance X-ray powder diffractometer with a Cu $\text{K}\alpha$ intensity of diffracted radiation within the range of 5°–60° as a function of the angle 2θ between the incident and diffracted beams. Electronic spectra of Schiff base ligand and their neat VO(IV) and/or Cu(II) complexes were recorded on 'SHIMADZU' UV-2450 spectrophotometer using quartz cell of 1 cm^3 optical path in 10^{-3} M methanol and DMF solutions, respectively. However, the UV reflectance spectra of zeolite-Y entrapped complexes were recorded on UV reflectance spectrometer (Model: LAMDA 19 UV/VIS/NIR) in the solid phase at room temperature. Thermogravimetric (TG) analysis of ligand, their neat as well as entrapped complexes were carried out in air atmosphere in the temperature range 40–700 °C using Shimadzu TGA-50 Instrument.



SCHEME 1 The plausible mechanism for BV oxidation of cyclopentanone using $[VO(L)H_2O]-Y$ catalyst

2.3 | Synthesis of Schiff base ligand (H_2L)

A methanolic solution (50 ml) of *o*-amino phenol (6.0 g, 0.055 M) and salicylaldehyde (6.71 g, 0.055 M) in 1:1 molar ratio was mixed with constant stirring. Refluxing was carried out for 4 h. The solution was cooled overnight at room temperature. The formed orange-yellow colored crystals were collected and dried in air. Yield: 70%. Anal. Calcd. (%), C (73.23%), H(5.16%), N(6.57%); found (%) C(73.58%), H (5.07%), N(6.92%); 1H NMR (400 MHz, $DMSO-d_6$): δ (ppm) = 5.85 (1H, s, C-H of the lateral chain); 7.15–7.48 (m, for aromatic protons); 6.97–7.07 (4H, m, phenolic ring protons); 8.8 [1H, s, -OH---N (intra-molecular hydrogen bonding)]; 12.3 (1H, s, -OH); FTIR (KBr, cm^{-1}): (C = O) 1690, 1631 (C = N), 3045 (O–H) of phenolic ring, 1369 $\nu_{(C-O)}$; UV–vis (λ_{max} , nm) (transition): 290 (ILCT), 370 ($\pi \rightarrow \pi^*$), 422 ($n \rightarrow \pi^*$).

2.4 | Synthesis of transition metal complexes with Schiff base ligand (neat complexes)

To a solution of Schiff base ligand prepared in 10 mL of methanol, an equimolar methanolic solution of $VOSO_4 \cdot 5H_2O$ and/or $Cu(NO_3)_2 \cdot 3H_2O$ was added drop-wise in it. The pH of the clear solution was adjusted to 5–6 by drop-wise addition of CH_3COONa . The resultant mixture was refluxed for 4–5 h with constant stirring and was left for recrystallization. The solid product was separated by filtration and dried in vacuum.

2.5 | Synthesis of metal exchanged zeolites $[VO(IV)-Y$ or $cu(II)-Y$]

Metal exchanged zeolite was synthesized by heating neat zeolite (Na-Y) for 24 h at 250 °C to eradicate the impurities. 2 g of Na-Y was suspended in a round-bottom flask with 50 ml of 0.01 M aqueous solution of $VOSO_4 \cdot 5H_2O$ and/or $Cu(NO_3)_2 \cdot 3H_2O$, and the resultant mixture was refluxed with continuous stirring for 24 h at 90 °C. To prevent metal hydroxide preparation, the pH of the solution was maintained between 3 and 5. After 24 h, the solutions were filtered and washed thoroughly with warm deionized water to remove all dissolved ions or free from any metal ion content. The metal exchanged zeolite was then dried for 10 h in an oven at 120 °C for further use.

2.6 | Synthesis of zeolite-Y entrapped transition metal-Schiff base complexes

Zeolite-Y entrapped metal transition complexes were synthesized following the “Flexible ligand” method.^[37,38] In a general procedure, 1 g of activated metal substituted zeolite-Y $[VO(IV)-Y$ and/or $Cu(II)-Y$] was successively mixed with methanolic solution of ligand (H_2L , 25 mL) and refluxed with continuous stirring at 60 °C for 24 h under nitrogen atmosphere. The resulting solid powders so obtained were subjected to Soxhlet extraction for several hours using chloroform, acetonitrile, methanol and acetone as solvents. The color of the compounds did not alter after Soxhlet extraction and prolonged exposure to air, indicating the formation

of metal complexes inside zeolite-Y. The powders were then dried under vacuum and kept in a desiccator for further characterization.

2.7 | Catalytic BV oxidation of Cyclopentanone

The BV oxidation of cyclopentanone was tested to observe the effect of heterogeneous catalysts over homogeneous stuff. The catalytic reactions were carried out in a two-necked 50 ml round-bottom flask. Reaction conditions for the liquid-phase oxidation of cyclopentanone were as follows: cyclopentanone (3.54 ml, 0.04 mol), 30% H₂O₂ (2.34 ml, 0.1 mol) and catalyst (80 mg) were mixed in methanol (4 ml). The resulting mixture was then refluxed at 70 °C in an oil-bath for 6 h with continuous stirring. After filtration and washing with a solvent, the filtrate was subjected to gas chromatograph to analyze and identify the reaction products.

3 | RESULTS AND DISCUSSION

3.1 | Elemental analysis

The metal ion contents after entrapment can be assigned the presence of Schiff base complexes in the nanocavities of zeolite-Y. The chemical analysis data of neat and entrapped VO(IV) and/or Cu(II) based complexes are given in Table 1. The chemical analysis of the samples viz. [VO(L)H₂O]-Y and/or [Cu(L)H₂O]-Y revealed the presence of organic matter with a C/N ratio almost comparable with that of neat complexes. The analogous Si/Al ratio in all zeolite-Y based samples (Table 1), suggested the absence of dealumination process and the fortification of the zeolite-Y framework during the modification.

3.2 | BET surface area analysis

As presented in Table 2, a reduction in the BET surface area and pore volume of [VO(L)H₂O]-Y and/or [Cu(L)H₂O]-Y entrapped complexes observed upon the entrapment of complexes inside the nanovoids of pure zeolite-Y. This decreasing in BET surface area and pore volume clearly specifies the entrapment of metal complexes inside the supercages of

zeolite-Y. This observation not only confirms the presence of metal complexes within the nanovoids but also refutes the obliteration possibility of the zeolite-Y framework upon such modifications viz. ion exchange and the entrapment.

3.3 | SEM analysis

During the course of preparation of zeolite-Y entrapped metal complexes, an excessive amount of Schiff base ligand (H₂L) reacts with VO(IV)-Y and/or Cu(II)-Y (Section 2.6), the possibility of clumsy ligand and the formation of metal complex on the exterior surface of zeolite-Y cannot be debarred with the concurrent metal complex formation within the nanovoids of zeolite-Y. These peripheral particles can be easily seen in the SEM image of [VO(L)H₂O]-Y catalyst taken before [Figure 1(A)] the Soxhlet extraction. To circumvent the escaping of such superfluous particle from the exterior surface of zeolite-Y during the catalytic study, both the entrapped complexes of VO(IV) and/or Cu(II) are purified by Soxhlet extractor using assorted solvents like chloroform, acetonitrile, methanol and acetone until the filtrate becomes colorless and free from any metal ions. The SEM image of [VO(L)H₂O]-Y taken after the Soxhlet extraction [Figure 1 (B)] implies the existence of well-defined zeolite-Y crystals without any silhouette of the exterior redundant metal ions or the complexes. This corroborates that the morphology and surface crystallinity of zeolite-Y leavings undamaged upon the entrapment of the complexes.^[39]

3.4 | FTIR spectral analysis

FTIR spectra of Schiff base ligand (H₂L), VO(IV)-Y, Cu(II)-Y and their neat and entrapped complexes are illustrated in Figure 2 and are discussed here. FTIR spectra of VO(IV)-Y and Cu(II)-Y (Figure 2d, e) show a strong broad band at ~1070 cm⁻¹ due to the asymmetric stretching vibration of (Si/Al)O₄ units.^[40,41] Metal exchanged zeolites also show characteristic bands at ~457, ~831 and ~1174 cm⁻¹ (Figure 2d, e) and these bands were not modified on entrapment of the Schiff base metal complexes, indicating entrapment has not affected the zeolite framework (Figure 2 f, g). FTIR spectra of neat and entrapped complexes were harmonized with that of Schiff base ligand (H₂L) to define

TABLE 1 Chemical composition data of synthesized compounds

Compound	C (%)	H (%)	N (%)	M (%)	C/N	Si (%)	Al (%)	Si/Al
Na-Y	-	-	-	-	-	31.16	6.45	4.83
VO(IV)-Y	-	-	-	1.97	-	31.06	6.43	4.83
Cu(II)-Y	-	-	-	1.68	-	31.11	6.44	4.83
[VO(L)H ₂ O]	48.76 (48.65)	3.21 (3.15)	9.63 (9.46)	11.78 (11.47)	5.06 (5.14)	-	-	-
[VO(L)H ₂ O]-Y	1.98	0.74	0.37	1.95	5.35	30.97	6.41	4.83
[Cu(L)H ₂ O]-Y	1.65	0.77	0.32	1.66	5.15	30.89	6.40	4.83

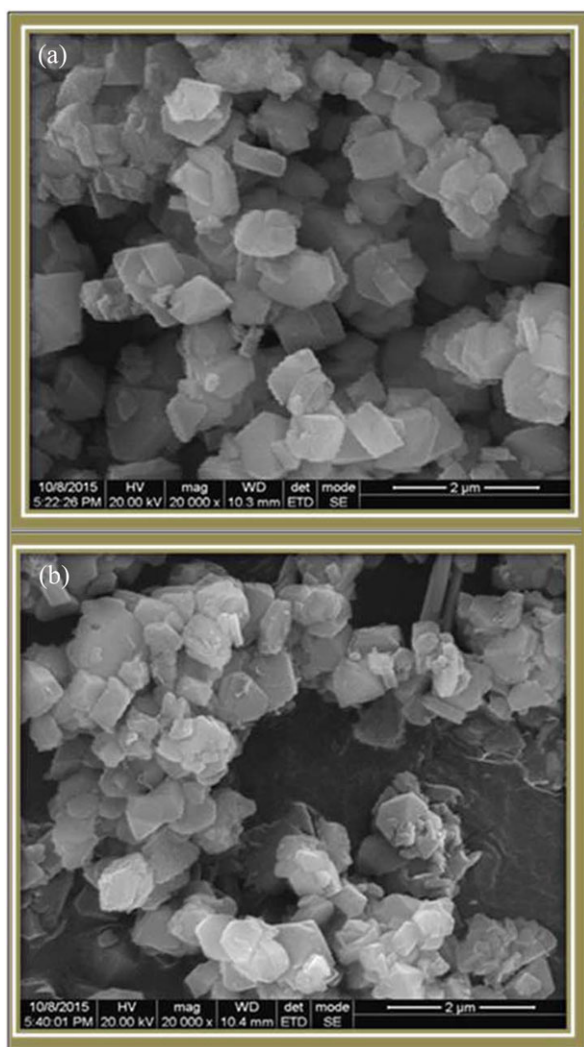
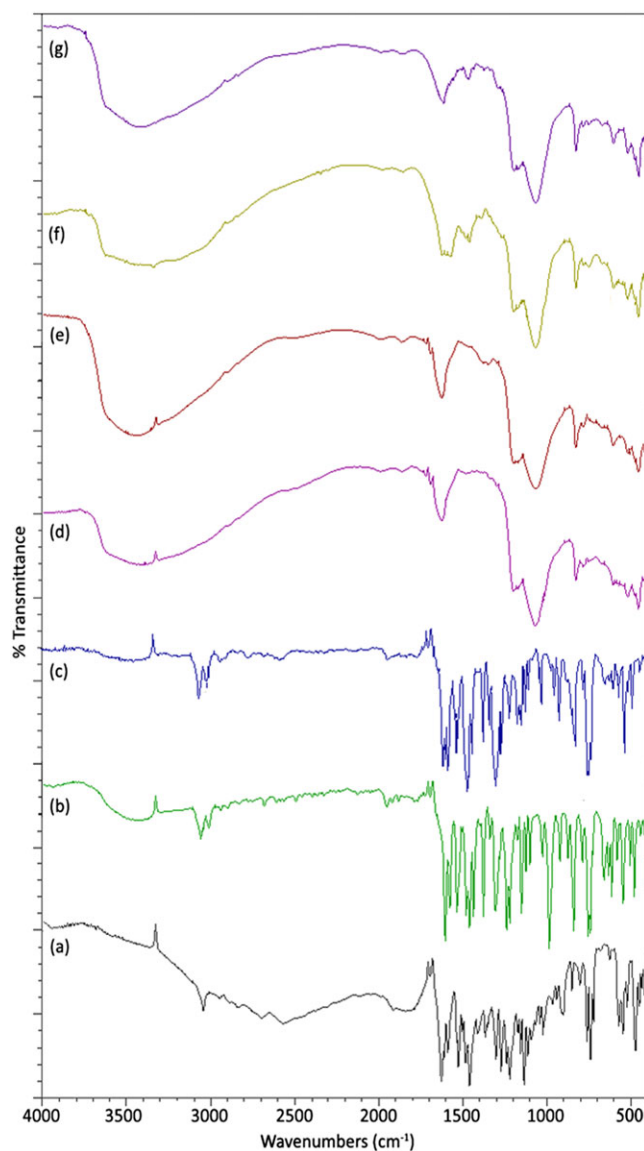
TABLE 2 Specific surface area measurement data^a

Compound	Specific surface area (m ² /g)	Specific pore volume (cm ³ /g)
Na-Y	600	0.32
VO(IV)-Y	544	0.29
Cu(II)-Y	531	0.28
[VO(L)H ₂ O]-Y	434	0.22
[Cu(L)H ₂ O]-Y	419	0.21

^aCalculated by the BJH-method.

the coordination sites which involved in chelation. The FTIR spectrum of Schiff base ligand (H₂L) exhibits a sharp band at 1631 cm⁻¹; which can be recognized by the vibration band of the azomethine group. Whilst in the spectra of neat and entrapped complexes, this band was shifted towards lower wave number and appears at 1610–1618 cm⁻¹, indicating that the coordination takes place through azomethine nitrogen. The FTIR spectra of neat complexes shown in Figure 2b, c exhibited the characteristic C = C, and C–O

stretching vibrations at ~1460, and ~1380 cm⁻¹, respectively. The presence of these bands, characteristic of ligand, duly confirms the formation of the metal Schiff base complexes, viz. [VO(L)H₂O], and [Cu(L)H₂O]. A broad band in the region ~3450 cm⁻¹, and two weaker bands at ~760 and ~560 cm⁻¹ in all neat and entrapped complexes are attributed

**FIGURE 1** SEM images of [VO(L)H₂O]-Y catalyst (a) before Soxhlet extraction (b) after Soxhlet extraction**FIGURE 2** FTIR spectra of (a) H₂L (b) [VO(L)H₂O] (c) [Cu(L)H₂O] (d) VO(IV)-Y (e) Cu(II)-Y (f) [VO(L)H₂O]-Y (g) [Cu(L)H₂O]-Y

to -OH stretching, rocking and wagging vibrations, respectively, which indicate the presence of coordinated water molecule.^[42] The thermal data confirms the nature of water molecule to be lattice or coordinated. The thermal study will be discussed in detailed manner later (Section 3.7). Neat VO(IV) complex exhibits a sharp band at 989 cm^{-1} due to $\nu(\text{V}=\text{O})$ stretching,^[43] while the position of such $\nu(\text{V}=\text{O})$ band in VO(IV)-Y and their entrapped complex was not possible may be due to the appearance of a strong and broad band in this region due to zeolitic frame work. Conclusive evidence regarding the bonding of protonated oxygens and azomethine nitrogen to the metal ion is provided by the occurrence of two new bands at ~ 525 and $\sim 450\text{ cm}^{-1}$ in the neat complexes, assigned to $\nu(\text{M}-\text{O})$ and $\nu(\text{M}-\text{N})$ modes, respectively. These data confirm the fact that Schiff base ligand behaves as a dinegative tridentate ligand forming a conjugated chelate ring, with the ligand existing in the complexes in the enolized form.

3.5 | X-ray powder diffraction studies

The powder X-ray diffraction patterns of Na-Y, VO(IV)-Y, Cu(II)-Y and their entrapped complexes are shown in figure. 3. The PXRD patterns of the Na-Y and VO(IV)-Y were almost comparable (Figure 3a and b, respectively). However, in the case of [VO(L)H₂O]-Y entrapped complex, the intensities of the I_{220} and I_{311} planes observed at 10° and 12° 2θ values

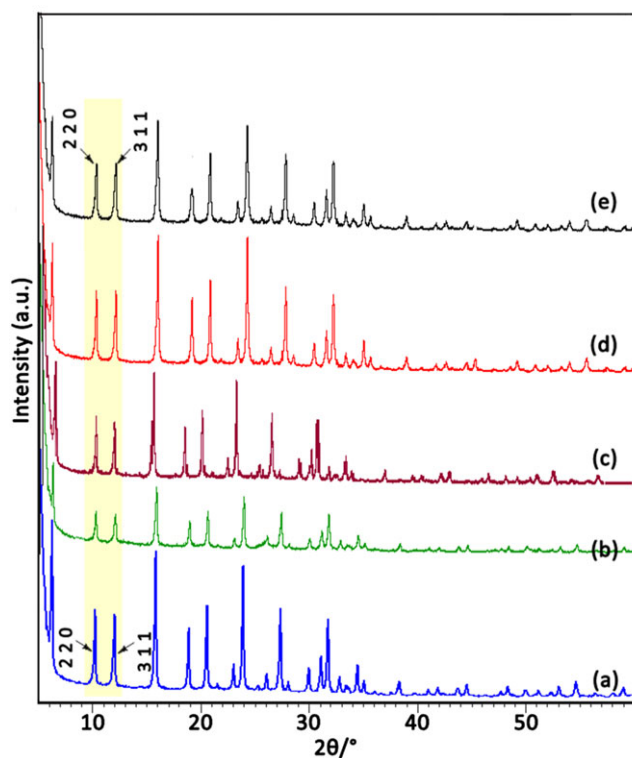


FIGURE 3 XRD patterns of (a) Na-Y (b) VO(IV)-Y (c) Cu(II)-Y (d) [VO(L)H₂O]-Y (e) [Cu(L)H₂O]-Y

became upturned (Figure 3d). In the case of Na-Y and VO(IV)-Y the intensity of the 220 plane was greater than that of the 311 plane; that is, $I_{220} > I_{311}$. Reversal of the intensities of the 220 and 311 planes, i.e. $I_{220} < I_{311}$, utterly divulges the formation of VO(IV)-Schiff base complex inside zeolite-Y.^[44,45] Such observations of the turnaround of the peak intensities in the zeolite-Y entrapped complexes were also made previously by various other researchers.^[29,46] We also observed such alterations in case of Cu(II) Schiff base complex incorporated inside zeolite-Y.

3.6 | Electronic spectra

Electronic spectra of Schiff base ligand (H₂L) and their VO(IV) and Cu(II) neat complexes were recorded in DMF solution and are shown in Figure 4, whereas zeolite-Y entrapped VO(IV) and/or Cu(II) complexes were recorded in the solid phase at room temperature and are illustrated in Figure 5. The electronic spectra of H₂L demonstrates three bands at 292, 352 and 430 nm owing to ILCT (intra ligand charge transfer transition), $\pi \rightarrow \pi^*$ and $n \rightarrow \pi^*$ transitions, respectively. In the spectra of neat VO(IV) and Cu(II) complexes, the value of the first band (ILCT transition) has undergone hypsochromic shift and appeared at shorter wavelength viz., 286 and 272 nm, respectively, resulting from the chelation of the ligand with the transition metal ions. However, the later two bands ($\pi \rightarrow \pi^*$ and $n \rightarrow \pi^*$ transitions) are as good as to the values for the discrete neat VO(IV) complex and are observed at 350 and 430 nm, respectively. Furthermore, $\pi \rightarrow \pi^*$ transition is remarkably akin to the values for the entrapped complexes observed at ~ 360 nm (Figure 5). This may indicate the immobilization of complexes within the nanopores of zeolite-Y.^[47]

The UV-reflectance spectra of VO(IV) entrapped complex shows two additional absorption bands at 585 and

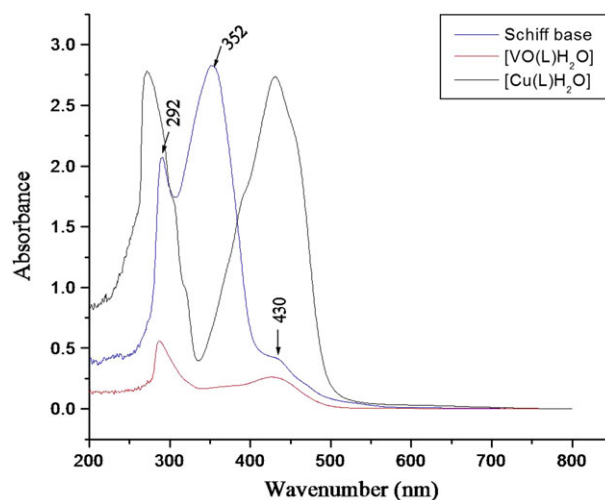


FIGURE 4 Electronic spectra of Schiff base ligand (H₂L) and their VO(IV) and Cu(II) neat complexes

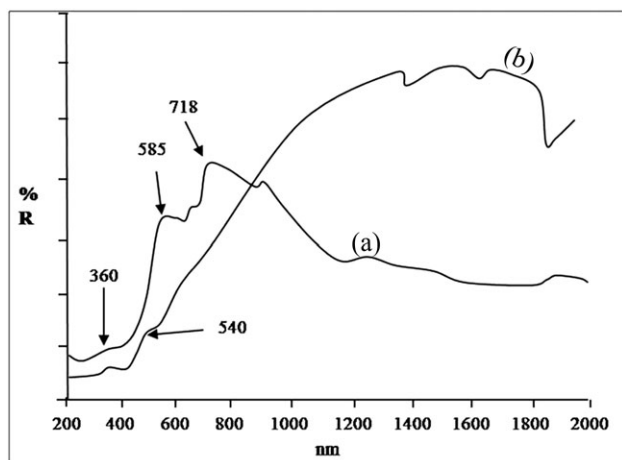


FIGURE 5 UV reflectance spectra of (a) [VO(L)H₂O]-Y (b) [Cu(L)H₂O]-Y

718 nm may be attributed to $b_2 \rightarrow b_1$ and $b_2 \rightarrow e$ transitions, respectively,^[48] suggesting the square pyramidal (C_{4v}) geometry of this complex. On the other hand, the reflectance spectrum of zeolite-Y entrapped Cu(II) complex shows a shoulder at 540 nm, may be allocated to ${}^2A_{1g}(F) \rightarrow {}^2B_{1g}(P)$ $d-d$ transition, implying a square-planar geometry around the Cu(II) ion.^[49]

3.7 | TG analysis

TG report of as prepared samples viz., H₂L, neat [VO(L)H₂O], [VO(L)H₂O]-Y and [Cu(L)H₂O]-Y is represented in Figure 6. The thermogravimetric analysis data in accordance with the percent weight loss in different phases and their possible assignments are presented in Table 3.

The decomposition of ligand (H₂L) takes place in two phases (Figure 6(a)). In the first phase, practically 53.11%

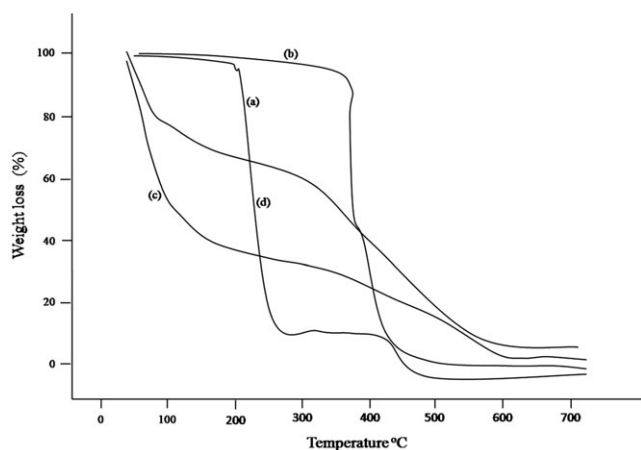


FIGURE 6 TG Curves of (a) H₂L (b) [VO(L)H₂O] (c) [VO(L)H₂O]-Y (d) [Cu(L)H₂O]-Y

of weight loss is detected in the range 50–220 °C, due to the initial breakdown of ligand. In the second phase, 46.88% of weight loss is detected in the range 220–460 °C due to absolute subtraction of ligand might be due to formation of gases like CO, CO₂, NO, NO₂.^[1]

As shown in Figure 6(b), the neat [VO(L)H₂O] complex decomposes in two phases. During the first phase, thermal dehydration of coordinated water molecule from this complex takes place between 50–200 °C, with a mass loss of 5.84% (calc. 6.08%). One mole of coordinated water molecule is removed in this stage of dehydration. In the second phase, neat complex decomposes within the temperature range of 200–700 °C with the estimated weight loss of 66.02% (cal. 65.89%), attributed to the elimination of ligand via complex breakdown and leaving behind VO₂ as the final residue (Table 3).

As shown in Figure 6 (c) and (d), the thermal decomposition of [VO(L)H₂O]-Y and [Cu(L)H₂O]-Y mainly occurs in the temperature range of 50–200 °C with a mass loss of 15.88 and 14.38%, respectively, owing to the exclusion of physically and chemisorbed water molecules from the zeolite framework.^[50] In the second phase experiences the weight loss of 25.26% and 14.38%, respectively in the wide range of 200–700 °C, can be allotted to the loss of the chelating ligand which signifies the presence of only small amounts of the metal complex in the nanovoids of the zeolite Y (Table 3). From the above discussions, a square-pyramidal structure for neat [VO(L)H₂O] complex and a square-planar structure for [Cu(L)H₂O] complex can tentatively be assumed as shown in Figure 7.

4 | CATALYTIC STUDIES

Usually, the BV oxidation of cyclopentanone shows the way of fabrication of its selective product i.e., δ -valerolactone. In this work, reaction conditions were optimized to control the liquid-phase BV oxidation of cyclopentanone. To acquire this, primarily, all the catalysts, including Na-Y, metal exchanged zeolitic samples, neat and zeolite Y entrapped metal complex samples were experienced for this BV oxidation of cyclopentanone (Table 4). Samples taken at regular time intervals were analyzed by GC. Based on these experimentations, [VO(L)H₂O]-Y was taken as representative catalyst as it shown notable catalytic activity (Table 4). in the form of conversion of cyclopentanone (80.22%) and δ -valerolactone selectivity (83.56%) along with remarkable TOF (1746.76 h⁻¹) and TON (10479.42) values, and hence, it was preferred as a representative catalyst to check the impact of experimental variables such as impact of varying mole ratio, amount of catalysts, reaction time, varying oxidants, varying solvents on cyclopentanone oxidation as described below:

TABLE 3 Thermogravimetric results of H₂L, their neat and zeolite-Y entrapped complexes

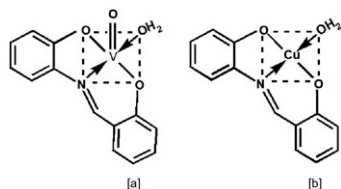
Compound	TG range (°C)	Mass loss (%) obs. (calc.)	Assignment
H ₂ L	50–220 220–460	53.11 46.88	Removal of one part of the ligand Removal of remaining part of the ligand
[VO(L)H ₂ O]	50–200 200–700	5.84 (6.08) 66.02 (65.89) 71.84* (71.97)	Loss of one coordinated water molecule Removal of Schiff base ligand Leaving VO ₂ as residue
[VO(L)H ₂ O]-Y	50–200 200–700	15.88 25.26	Loss of intrazeolite + coordinated water molecules Loss of Schiff base ligand
[Cu(L)H ₂ O]-Y	50–200 200–700	16.03 14.38	Loss of intrazeolite + coordinated water molecules Loss of Schiff base ligand

4.1 | Impact of varying mole ratio on oxidation of cyclopentanone

Four different mole ratios (1:1, 1:1.5, 1:2, 1:2.5) of cyclopentanone to 30% H₂O₂ were taken to determine their effect on cyclopentanone oxidation by keeping all other reaction parameters fixed. Conversion of cyclopentanone was improved from 80.22 to 97.99% upon increasing the mole ratio of cyclopentanone to 30% H₂O₂ from 1:1 to 1:2.5, respectively (Table 5). On the other hand, the rate of selectivity of δ -valerolactone decreased from 83.56 to 80.99% as the ratio was increased from 1:1 to 1:2.5. It may be due to decomposition of H₂O₂ forming large amount of water, which will cause the selectivity of δ -valerolactone via hydrolysis reaction to form 5-hydroxypentanoic acid. Consequently, the molar ratio was taken to be 1:1 to conduct further experimentation.

4.2 | Impact of varying amount of catalyst on oxidation of cyclopentanone

The amount of catalyst was crucial to the conversion of the heterogeneous catalyzed oxidation of cyclopentanone along with δ -valerolactone selectivity. Values of cyclopentanone conversion and δ -valerolactone selectivity are given in Table 6 for typical essays. Escalating the amount (from 40 to 80 mg) of [VO(L)H₂O]-Y catalyst results in higher conversion of cyclopentanone along with δ -valerolactone selectivity, i.e. conversion and selectivity enhances from 16.42 to 80.22 and 55.87 to 83.56, respectively. While further raising the catalyst amount (up to 100 mg), the selectivity of δ -valerolactone decreased. This change may be due to increase

**FIGURE 7** The proposed structures of (a) [VO(L)H₂O] (b) [Cu(L)H₂O]

in amount of the radical formation, whereby the rate of selectivity decreased. Consequently, the optimum catalyst dosage considered to be 80 mg to conduct further experimentation.

4.3 | Impact of varying reaction time on oxidation of cyclopentanone

To regulate the crucial reaction time, catalytic BV oxidation was examined at varying time i.e. 6, 8, 12 and 24 h. It was observed that cyclopentanone conversion increased with time growing and reached the top at 24 h with 11854.93 TONs (Table 7). However, the selectivity was decreased to some extent with time, owing to the decomposition of H₂O₂. With escalating reaction time from 6 to 24 h, low selectivity of δ -valerolactone (from 83.56 to 83.44%) was observed. It might be due to the further hydrolysis of δ -valerolactone to pentanoic acid.^[51] It meant that the reaction time was one of influencing factor for BV oxidation of cyclopentanone, and consequently the optimum reaction time considered to be 6 h.

4.4 | Impact of varying oxidant on oxidation of cyclopentanone

Two different oxidant systems viz., TBHP and/or H₂O₂ were studied over [VO(L)H₂O]-Y catalyst to determine their effect on cyclopentanone oxidation by keeping all other reaction parameters fixed. The results obtained over the catalyst at different oxidant systems are tabulated in Table 8. Though TBHP is strong oxidant than H₂O₂, in our case, we found high conversion of cyclopentanone (80.22%) with H₂O₂ and higher selectivity of δ -valerolactone (83.56%) as well. H₂O₂ is one of the technologically green oxidant, due to the innocuous nature of its by-product, water. As stated in Scheme 1, the activation of the catalyst, [VO(L)H₂O]-Y occurs by the reaction with H₂O₂ forming HOOV^VOH(L) species.^[52] In this species, the O–O bond is polarized, facilitating the hydroxyl group labile to attack the nucleophilic ketone carbonyl group of cyclopentanone and gives the final product, δ -valerolactone.

TABLE 4 Catalytic performance of synthesized materials over BV oxidation of cyclopentanone

Compound	Cyclopentanone conversion (%)	Selectivity (%) δ -valerolactone	TOF ^a (h ⁻¹)	TON ^b
Na-Y	8.49	80.12	-	-
VO(IV)-Y	42.23	84.11	-	-
Cu(II)-Y	40.92	83.99	-	-
[VO(L)H ₂ O]	70.16	83.28	252.82	1516.92
[Cu(L) H ₂ O]	44.55	83.18	-	-
[VO(L)H ₂ O]-Y	80.22	83.56	1746.76	10479.42
[Cu(L) H ₂ O]-Y	50.40	83.76	1608.42	9650.52

Reaction condition: 80 mg catalyst, 4 mL methanol, 0.04 mol cyclopentanone, 0.1 mol 30% H₂O₂, 70 °C, 6 h.

^aTOF: moles of phenol converted per mole of metal per hour

^bTON: moles of phenol converted per mole of metal

TABLE 5 Impact of varying molar ratio (cyclopentanone/H₂O₂) on oxidation of cyclopentanone

Compound	Cyclopentanone/ H ₂ O ₂ (%)	Cyclopentanone conversion (%)	Selectivity (%) δ -valerolactone	TOF (h ⁻¹)	TON
[VO(L)H ₂ O]-Y	1:1	80.22	83.56	1746.76	10479.42
[VO(L)H ₂ O]-Y	1:1.5	89.54	83.13	1810.13	10860.75
[VO(L)H ₂ O]-Y	1:2	90.12	82.68	1962.33	11773.98
[VO(L)H ₂ O]-Y	1:2.5	97.99	80.99	2133.69	12802.18

Reaction condition: 80 mg [VO(L)H₂O]-Y as a representative catalyst, 4 ml methanol, 0.04 mol cyclopentanone, 70 °C, 6 h.

TABLE 6 Impact of varying amount of catalyst on oxidation of cyclopentanone

Compound	Amount of catalyst (mg)	Cyclopentanone conversion (%)	Selectivity (%) δ -valerolactone	TOF (h ⁻¹)	TON
[VO(L)H ₂ O]-Y	40	16.42	55.87	357.54	2145.23
[VO(L)H ₂ O]-Y	60	18.7	44.36	407.19	2443.11
[VO(L)H ₂ O]-Y	80	80.22	83.56	1746.76	10479.42
[VO(L)H ₂ O]-Y	100	83.14	80.21	1810.34	10862.06

Reaction condition: cyclopentanone (0.04 mol), 30% H₂O₂ (0.04 mol), 70 °C, 6 h, catalyst 80 mg, methanol 4 ml.

TABLE 7 Impact of varying time on oxidation of cyclopentanone

Sr. No.	Time (h)	Cyclopentanone conversion (%)	Selectivity (%) δ -valerolactone	TOF (h ⁻¹)	TON
1	6	80.22	83.56	1746.76	10479.42
2	8	85.36	82.11	1858.68	11152.09
3	12	86.17	83.15	1876.32	11257.92
4	24	90.74	83.44	1975.83	11854.93

Reaction condition: cyclopentanone (0.04 mol), 30% H₂O₂ (0.04 mol), 70 °C, catalyst 80 mg, methanol 4 ml.

TABLE 8 Impact of varying oxidant on oxidation of cyclopentanone

Sr. No.	Oxidant	Cyclopentanone conversion (%)	Selectivity (%) δ -valerolactone	TOF (h ⁻¹)	TON
1	H ₂ O ₂	80.22	83.56	1746.76	10479.42
2	TBHP	47.52	79.81	1034.73	6208.38

Reaction condition: cyclopentanone (0.04 mol), 70 °C, catalyst 80 mg, methanol 4 ml, 6 h.

4.5 | Impact of varying solvents on oxidation of cyclopentanone

In the present study, three different solvents were used with [VO(L)H₂O]-Y catalyst to perceive their effect on BV

oxidation of cyclopentanone (Table 9). The cyclopentanone conversion obtained with different solvent decreases in the order, methanol (80.22%) > acetonitrile (25.15%) > 1,4-dioxane (12.45%). Methanol shows higher TOF (1746.76 h⁻¹) and TON (10479.42) though it is difficult to describe that

TABLE 9 Impact of varying solvent on oxidation of cyclopentanone

Catalyst	Cyclopentanone conversion (%)	Selectivity (%) δ -valerolactone	TOF (h^{-1})	TON
Acetonitrile	25.15	55.87	547.63	3285.79
1,4-dioxane	12.45	44.36	271.09	1626.56
Methanol	80.22	83.56	1746.76	10479.42

Reaction condition: cyclopentanone (0.04 mol), 30% H_2O_2 (0.04 mol), 70 °C, catalyst 80 mg, 6 h.

which goods of the solvent influenced the cyclopentanone conversion. However, it may be due to inductive effect; the electron cloud of oxygen atom in methanol can activate the ketone carbonyl group of the cyclopentanone via transferring to vacant electron site of vanadium, and thus enhancement of electrophilicity of ketone carbonyl oxygen. Thus, increase of electrophilicity can favor oxidation reaction.^[53,54] On the other hand, due to the lack of the proton donating group, the non-protic solvents, such as acetonitrile and 1,4 dioxane, cannot increase stability of intermediate and hence they have lower reaction activity.

4.6 | Baeyer-Villiger oxidation of cyclic ketones

Under the best reaction conditions, various cyclic ketones (0.04 mol) reacted with representative catalyst, [VO(L)H₂O]-Y (80 mg), 30% H_2O_2 (0.04 mol) in methanol (4 ml) to give corresponding lactone products at 70 °C (Table 10). The reaction of cyclopentanone and cyclohexanone gave the corresponding products 84–85% yields with observed TOF (1746.76 and 1238.99 h^{-1} , respectively) and TON (10479.42 and 7433.94, respectively) values.

4.7 | Recyclability test

A series of recyclability tests were performed to check the efficiency of [VO(L)H₂O]-Y catalyst on BV oxidation of cyclopentanone (Table 11). Fresh [VO(L)H₂O]-Y catalyst has shown 80.22% conversion of cyclopentanone with 83.56% selectivity towards δ -valerolactone. Additionally, it

TABLE 10 Baeyer-Villiger oxidation of cyclic ketones

Substrate	Product	Conversion (%)	Selectivity (%)	TOF (h^{-1})	TON
		80.22	83.56	1746.76	10479.42
		56.87	84.67	1238.99	7433.94

Reaction condition: Substrate (0.04 mol), 30% H_2O_2 (0.04 mol), 70 °C, [VO(L)H₂O]-Y catalyst 80 mg, methanol 4 ml, 6 h.

was recycled and washed with methanol after each run and dried at 110 °C for the BV oxidation of cyclopentanone with a view to establishing the effect of entrapment on thermal stability, catalytic activity, and reusability. Under the same reaction conditions, the catalytic activity in consecutive runs has no or minor apparent reduction as compared to the fresh catalyst with 81.72, 75.92, and 74.46% δ -valerolactone selectivity for three consecutive runs, respectively (Figure 8). For this reason, it is impeccable to say that the porous support prevents the complex from leaching and decomposition during the reaction, and makes it recyclable and reusable.

4.8 | Catalytic assessment

X. Peng and his group^[55] reported the BV oxidation of cyclopentanone over silica/A153-SO₃H catalyst (Table 12, entry 2). They observed maximum conversion of cyclopentanone (53%) and δ -valerolactone selectivity of 45% with acetonitrile solvent system. Catalyst Sn-aminomethyl polystyrene was developed by Q. Zhang *et al.*^[56] and used to check over Baeyer-Villiger oxidation of cyclopentanone. This catalytic system allowed converting the substrate 22% only with lactone selectivity of 100% using fluorobenzene as a solvent system along with low TON value of 58 (Table 12, entry 3). Y. Wang *et al.*^[57] developed a catalytic system involving polar hydrophilic Fe-Co/SO₃H head group and a hydrophobic PS tail, i.e., Fe-Co/SPS system, achieving 81% conversion of cyclopentanone with nearly similar δ -valerolactone selectivity (80%) in CH₂Cl₂ as a solvent (Table 12, entry 4). Z. Lei and his co-workers^[58] focused on cyclic & acyclic ketones and the traditional Baeyer-Villiger oxidation using Aniline-Sn catalyst in 1,4-dioxane solvent system. They observed that this catalytic system is less promising for Baeyer-Villiger oxidation of

TABLE 11 Recyclability test of the recovered catalyst on the oxidation of cyclopentanone

Catalyst	Cyclopentanone conversion (%)	Selectivity (%) δ -valerolactone
Fresh	80.22	83.56
1st run	78.45	81.72
2nd run	72.69	75.92
3rd run	68.73	74.46

Reaction condition: cyclopentanone (0.04 mol), 30% H_2O_2 (0.04 mol), 70 °C, catalyst 80 mg, 6 h.

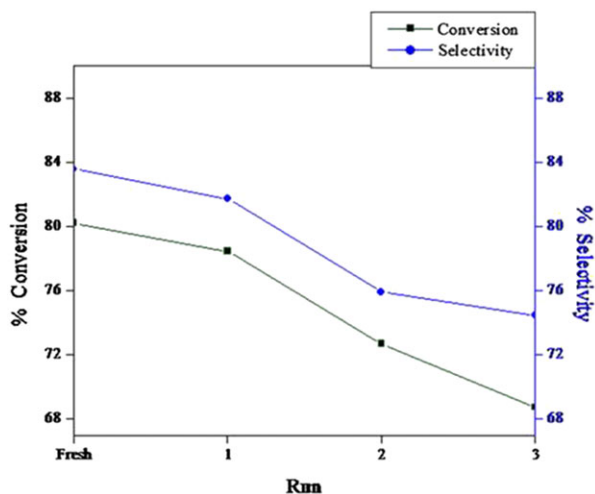


FIGURE 8 Recyclability of [VO(L)H₂O]-Y on oxidation of cyclopentanone

cyclopentanone with 60% conversion (Table 12, entry 5), while for other cyclic and acyclic ketones, promising conversion with 100% selectivity were observed. An admirable conversion of 100% and δ -valerolactone selectivity of >99% (Table 12, entry 6) in the BV oxidation of cyclopentanone was achieved by S. Konera *et al.*^[59] with tin-salen moiety immobilized into NaY zeolite matrix, i.e., Sn(salen)-NaY. Montmorillonite (MMT) supported Sn catalyst was prepared by Z. Lei *et al.*^[60] using ion-exchange technique (Table 12, entry 7). Cyclopentanone is oxidized by 30% H₂O₂ in n-Butanol solvent system over Sn-MMT catalyst achieving 45% conversion and 100% lactone selectivity (TON: 75). While in the present work (Table 12, entry 1), BV oxidation of cyclopentanone using 30% H₂O₂ as an oxidant carried

out over [VO(L)H₂O]-Y catalyst, gave very promising results of 80.22% conversion with 83.56% δ -valerolactone selectivity in 6 hours at 70 °C (TOF: 1746.76 h⁻¹ and TON: 10479.42).

4.9 | Proposed Catalytic mechanism of BV oxidation of cyclopentanone over [VO(L)H₂O]-Y catalyst:

Generally, inserting oxygen to an organic substrate in a distinctive Baeyer-Villiger oxidation reaction on an industrial scale would prefer a cheaper and eco-friendly source of oxidant i.e. H₂O₂ and/or O₂.

The mechanism of homogeneously catalyzed heterogenized Baeyer-Villiger oxidation of cyclopentanone is proposed in Scheme 1. In view of the catalyst being regenerated after a cycle of reactions, it should be possible to represent a catalytic process by a closed loop incorporating various steps of reactions involved. The mechanism can be broadly divided into two catalogues,^[61] one being activation of V^{IV} species (catalyst) that takes place through the electrophilic attack of H₂O₂ and other being activation of ketone carbonyl substrate through active intermediate species that will be discussed thoroughly as follows:

4.10 | Activation of V^{IV} species (catalyst) through the electrophilic attack of H₂O₂:

The Gibbs activation barriers for the addition and rearrangement steps in the non-catalyzed BV oxidation have been reported to be 39.8 and 41.7 k cal mol⁻¹, respectively, which makes the reaction difficult to proceed without catalyst.^[62,63]

TABLE 12 Comparison between reported heterogeneous catalytic systems and our catalyst for BV oxidation of cyclopentanone

Entry	Catalyst	Cyclopentanone conversion (%)	Solvent	TON ^a	TOF ^b (h ⁻¹)	Selectivity (%) δ -Valerolactone	Ref.
1	[VO(L)H ₂ O]-Y ^c	80.22	Methanol	10479.42	1746.76	83.56	This work
2	Silica/A153- SO ₃ H ^d	53	Acetonitrile	-	-	45	[51]
3	PS-Sn ^e	22	Fluorobenzene	58	-	100	[52]
4	Fe-Co/SPS ^f	81	CH ₂ Cl ₂	-	-	80	[53]
5	Aniline-Sn ^g	60	1,4-Dioxane	-	-	100	[54]
6	Sn(salen)-NaY ^h	100	1,4-Dioxane	-	158	>99	[55]
7	Sn-MMT ⁱ	45	n-Butanol	75	-	100	[56]

^aTON: Turnover number = moles converted/mol of active site.

^bTOF: Turnover frequency = moles converted/ (moles of active site \times time).

^cCyclopentanone (0.04 mol), 30% H₂O₂ (0.04 mol), methanol (4 ml), catalyst (80 mg), 70 °C, 6 h.

^dCyclopentanone (2.5 mmol), 30% H₂O₂ (1.5 ml), acetonitrile (3.0 mL), catalyst (10 mg), 10 °C, 20 h.

^eCyclopentanone (0.1 mmol), 30% H₂O₂ (1.5 eq to substrate), catalyst (4 mg), Fluorobenzene (3-ml) 70 °C, 24 h.

^fCyclopentanone (2.5 mmol), H₂O₂ (2.5 eq), catalyst (15 mg), 10 °C, 20 h.

^gCyclopentanone (0.1 mol), 30% H₂O₂ (1.5 eq), catalyst (2000 mg), 1,4-dioxane (3 ml), 70 °C, 12 h.

^hCyclopentanone (1000 mg), tert-BuOOH (2 ml), 1,4-dioxane (5 ml), catalyst (50 mg), 70 °C, 12 h.

ⁱCyclopentanone (0.1 mmol), 30% H₂O₂ (2.0 eq), catalyst (3 mg), n-Butanol (3 ml) 90 °C, 24 h.

By employing [VO(L)H₂O]-Y catalyst, the Gibbs activation barriers for the addition and rearrangement steps presumed to be reduced may be due to the activation of V^{IV} species [A] through the electrophilic attack of H₂O₂ (Step-I) followed by the formation of intermediate species, HOOV^{IV}OH(L) [B]. Upon rearrangement of this intermediate, an active species, •OOV^{IV}(L) [C] is formed.

4.11 | Activation of ketone carbonyl substrate and BV rearrangement of Criegee's intermediate to the lactone product:

The electrophilicity enhancement of ketone carbonyl facilitates the free radical attack via •OOV^{IV}(L) intermediate species [C]. In this reductive elimination step, this activated species, •OOV^{IV}(L), attacks the substrate reversibly, may be through interaction between the carbonyl group of the substrate and the Lewis acid sites (i.e., the metal atom incorporated in the zeolite lattice) with forming 'Criegee' intermediate, [D], which gives the final desired product (δ-valerolactone).

5 | CONCLUSIONS

- To sum up, synthesis of zeolite-Y entrapped metal complexes has been done efficiently as evidenced by various physico-chemical techniques viz., elemental analysis, BET, electronic and reflectance, FTIR, powder XRD, SEM, and thermogravimetric studies.
- The catalytic behavior of both the synthesized materials viz. homogeneous and heterogeneous systems (neat and entrapped complexes) has been tested over BV oxidation of cyclopentanone.
- Factors (the molar ratio of substrate to oxidant, catalyst amount, reaction time, oxidants, and solvents) that influence the oxidation were also thoroughly checked and optimum reaction conditions were improved as 0.04 mol cyclopentanone, 0.04 mol 30% H₂O₂, 80 mg [VO(L)H₂O]-Y catalyst, 4 mL methanol, 70 °C, 6 h.
- [VO(L)H₂O]-Y showed optimal performance by providing 10479.42 TONs (80.22% cyclopentanone conversion; 83.56% δ-valerolactone selectivity).
- The plausible catalytic cycle for the Baeyer-Villiger oxidation of cyclopentanone (Scheme 1) involved the following sequence of key steps:
- Activation of catalyst through the electrophilic attack of H₂O₂.
- Activation of ketone carbonyl substrate followed by BV rearrangement of Criegee's intermediate to obtain lactone product.
- The field of heterogeneous catalysis will be having ample of benefits over homogeneous system as it is

noteworthy for the handling, separation and recycling abilities from an inexpensive, technological and ecological point of view.

ACKNOWLEDGMENTS

We express our gratitude to the Head, Applied Chemistry Department, Faculty of Technology & Engineering, The Maharaja Sayajirao University of Baroda, Vadodara, Gujarat (India) for providing the necessary laboratory facilities. One of the authors (Chetan K Modi) would like to present his deep thanks and gratitude to the UGC, New Delhi [Grant F. No. 42-290/2013 (SR) dated-25 March 2013] for Major Research Project (MRP) financial support.

REFERENCES

- [1] J. P. Mehta, D. K. Parmar, D. R. Godhani, H. D. Nakum, N. C. Desai, *J. Mol. Catal. A: Chem.* **2016**, *421*, 178.
- [2] M. R. Maurya, U. Kumar, I. Correia, P. Adão, J. C. Pessoa, *Eur. J. Inorg. Chem.* **2008**, *4*, 577.
- [3] M. S. Niasari, A. Sobhani, *J. Mol. Catal. A: Chem.* **2008**, *285*, 58.
- [4] X. F. Zhou, *RSC Adv.* **2014**, *4*, 27857.
- [5] A. Corma, T. M. Navarro, M. Renz, *J. Catal.* **2003**, *219*, 242.
- [6] L. J. Davies, P. McMorn, D. Bethell, P. C. B. Page, F. King, F. E. Hancock, G. J. J. Hutchings, *J. Mol. Catal. A: Chem.* **2001**, *165*, 243.
- [7] A. Corma, M. T. Navarro, L. T. Nemeth, M. Renz, *Chem. Commun.* **2001**, 2190.
- [8] A. Corma, S. Iborra, M. Mifsud, M. Renz, *ARKIVOC* **2005**, 124.
- [9] C. K. Modi, P. M. Trivedi, *J. Coord. Chem.* **2014**, *67*, 3678.
- [10] L. Saikia, D. Srinivas, P. Ratnasamy, *Appl. Catal. A Gen.* **2006**, *309*, 144.
- [11] A. Corma, L. T. Nemeth, M. Renz, S. Valencia, *Nature* **2001**, *412*, 423.
- [12] Y. F. Li, M. Q. Guo, S. F. Yin, L. Chen, Y. B. Zhou, R. H. Qiu, C. T. Au, *Carbon* **2013**, *55*, 269.
- [13] *Ullmann's Encyclopedia of Industrial Chemistry*, 6th ed., Wiley-VCH, Weinheim **2002**.
- [14] G. J. Brink, I. W. C. E. Arends, R. A. Sheldon, *Chem. Rev.* **2004**, *104*, 4105.
- [15] P. Kraft, *Macrocyclic Lactones as Fragrances*, World Intellectual Property Organization 2012. WO/2009/039675, European Patent EP 2205581.
- [16] M. Weigele, M. F. Loewe, *Lactones and Their Pharmaceutical Applications*, World Intellectual Property Organization 1994. WO/1994/017056.
- [17] Y. Peng, X. Feng, K. Yu, Z. Li, Y. Jiang, C. H. Yeung, *J. Organomet. Chem.* **2001**, *619*, 204.
- [18] L. Zhou, X. Liu, J. Ji, Y. Zhang, X. Hu, L. Lin, X. Feng, *J. Am. Chem. Soc.* **2012**, *134*, 17023.

- [19] L. Zhou, X. Liu, J. Ji, Y. Zhang, W. Wu, Y. Liu, L. Lin, X. Feng, *Org. Lett.* **2014**, *16*, 3938.
- [20] S. Xu, Z. Wang, X. Zhang, X. Zhang, K. Ding, *Angew. Chem. Int. Ed.* **2008**, *47*, 2840.
- [21] N. Friess, N. Famham, *J. Am. Chem. Soc.* **1950**, *72*, 5518.
- [22] G. R. Krow, in *Comprehensive Organic Synthesis*, (Eds: B. M. Trost, I. Fleming) Vol. 7, Pergamon Press, Oxford **1991** 671.
- [23] P. Arpentiner, F. Cavani, F. Trifiro, *The Technology of Catalytic Oxidations*, Editions TECHNIP, Paris **2001**.
- [24] J. P. Mehta, D. K. Parmar, D. R. Godhani, H. D. Nakum, N. C. Desai, *J. Porous Mater.* **2016**, *23*, 1507.
- [25] S. Baj, A. Chrobok, *Synth. Commun.* **2008**, *38*, 2385.
- [26] K. B. Szpakowski, K. Latham, C. J. Rix, J. M. White, *Inorg. Chim. Acta* **2011**, *376*, 628.
- [27] T. Hara, M. Hatakeyama, A. Kim, N. Ichikuni, S. Shimazu, *Green Chem.* **2012**, *14*, 771.
- [28] A. J. Kotlewska, F. Rantwijk, R. A. Sheldon, I. W. C. E. Arends, *Green Chem.* **2011**, *13*, 2154.
- [29] M. Sharma, B. Das, G. V. Karunakar, L. Satyanarayana, K. K. Bania, *J. Phys. Chem. C* **2016**, *120*, 13563.
- [30] K. N. Bhagya, V. Gayathri, *J. Porous Mater.* **2014**, *21*, 197.
- [31] H. S. Abbo, S. J. J. Titinchi, *Top. Catal.* **2010**, *53*, 1401.
- [32] C. K. Modi, P. M. Trivedi, S. K. Gupta, P. K. Jha, *J. Incl. Phenom. Macro. Chem.* **2012**, *74*, 117.
- [33] C. Naccache, Y. Ben Taarit, *Chem. Phys. Lett.* **1971**, *11*, 11.
- [34] C. K. Modi, P. M. Trivedi, J. A. Chudasama, H. D. Nakum, D. K. Parmar, S. K. Gupta, P. K. Jha, *Green Chem. Lett. Rev.* **2014**, *7*, 278.
- [35] C. K. Modi, B. G. Gade, J. A. Chudasama, D. K. Parmar, H. D. Nakum, A. L. Patel, *Spectrochim. Acta A* **2015**, *140*, 174.
- [36] C. K. Modi, J. A. Chudasama, H. D. Nakum, D. K. Parmar, A. L. Patel, *J. Mol. Catal. A: Chem.* **2014**, *395*, 151.
- [37] M. Mandal, V. Nagaraju, G. V. Karunakar, B. Sarma, B. J. Borah, K. K. Bania, *J. Phys. Chem. C* **2015**, *119*, 28854.
- [38] C. K. Modi, P. M. Trivedi, *Micropor. Mesopor. Mater.* **2012**, *155*, 227.
- [39] T. A. Alsalm, J. S. Hadi, O. N. Ali, H. S. Abbo, S. J. J. Titinchi, *Chem. Cent. J.* **2013**, *7*, 3.
- [40] K. K. Bania, R. C. Deka, *J. Phys. Chem. C* **2011**, *115*, 9601.
- [41] V. Arun, N. Sridevi, P. P. Robinson, S. Manju, K. K. M. Yusuff, *J. Mol. Catal. A: Chem.* **2009**, *304*, 191.
- [42] K. Nakamoto, *Infrared Spectra and Raman Spectra of Inorganic and Coordination Compounds, Part B: Application in Coordination, Organometallic, and Bioinorganic Chemistry*, 6th ed., Wiley Interscience, Hoboken, NJ **2009**.
- [43] M. Salavati-Niasari, *Inorg. Chim. Acta* **2009**, *362*, 2159.
- [44] E. G. Ferrer, M. V. Salinas, M. J. Correa, F. Vrdoljak, P. A. Williams, *Zeitschrift für Naturforschung B* **2005**, *60*, 305.
- [45] W. H. Quayle, J. H. Lunsford, *Inorg. Chem.* **1982**, *21*, 97.
- [46] D. R. Godhani, H. D. Nakum, D. K. Parmar, J. P. Mehta, N. C. Desai, *Micropor. Mesopor. Mater.* **2016**, *235*, 233.
- [47] B. Fan, W. Fan, R. Li, *J. Mol. Catal. A: Chem.* **2003**, *201*, 137.
- [48] E. G. Ferrer, M. V. Salinas, M. J. Correa, F. Vrdoljak, P. A. M. Williams, *Z. Naturforsch.* **2005**, *60b*, 305.
- [49] a) B. N. Figgis, *Introduction to Ligand Field*, Wiley, New York **1966**; b) A. B. P. Lever, *Inorganic Electronic Spectroscopy*, 2nd ed., Elsevier, Amsterdam **1984**.
- [50] H. Diegruber, P. J. Plath, G. Schulz-Ekloff, M. Mohl, *J. Mol. Catal.* **1984**, *24*, 115.
- [51] J. Q. Bond, D. M. Alonso, R. M. West, J. A. Dumesic, *Langmuir* **2010**, *26*, 16291.
- [52] S. Parihar, S. Pathan, R. N. Jadeja, A. Patel, V. K. Gupta, *Inorg. Chem.* **2011**, *51*, 1152.
- [53] V. Arca, A. B. Boscoletto, N. Fracasso, L. Medab, G. Ranghino, *J. Mol. Catal. A: Chem.* **2006**, *243*, 264.
- [54] J. C. van der Waal, H. van Bekkum, *J. Mol. Catal. A: Chem.* **1997**, *124*, 137.
- [55] X. Peng, W. Xing, Q. Ma, *C.R. Chimie* **2015**, *18*, 581.
- [56] Q. Zhang, S. Wen, Z. Lei, *React. Funct. Polym.* **2006**, *66*, 1278.
- [57] Y. Wang, J. Huang, X. Xia, X. Peng, *J. Saudi Chem. Soc.* **2016**, <https://doi.org/10.1016/j.jscs.2016.01.006>.
- [58] Q. H. Zhang, S. F. Wang, Z. Q. Lei, *Chinese Chem. Lett.* **2007**, *18*, 4.
- [59] B. Dutta, S. Jana, S. Bhunia, H. Honda, S. Koner, *Appl. Catal. A: Gen.* **2010**, *382*, 90.
- [60] Z. Lei, G. Ma, C. Jia, *Catal. Commun.* **2007**, *8*, 305.
- [61] X. Cui, J. Shi, *Sci. China Mater.* **2016**, *59*, 675.
- [62] R. R. Sever, T. W. Root, *J. Phys. Chem. B* **2003**, *107*, 10848.
- [63] R. R. Sever, T. W. Root, *J. Phys. Chem. B* **2003**, *107*, 10521.

How to cite this article: Modi CK, Solanki N, Vithalani R, Patel D. Baeyer-Villiger oxidation of cyclopentanone over zeolite Y entrapped transition metal-Schiff base complexes. *Appl Organometal Chem.* 2017:e3910. <https://doi.org/10.1002/aoc.3910>